

Multi-Year Climatology of Large-Scale Traveling Ionospheric Disturbances Observed with High Frequency Amateur Radio Receiving Networks Using a Novel Automated Detection Algorithm

Diego Sanchez¹, Mary Lou West², Nathaniel A. Frissell¹, Mark Fenner¹, Gareth Perry³, V. Lynn Harvey⁴, Bill Engelke⁵, Nicholas W. Callahan, Philip J. Erickson⁶, Robert B. Gerzoff⁷
¹The University of Scranton ²Montclair State University ³New Jersey Institute of Technology ⁴University of Colorado Boulder ⁵University of Alabama ⁶MIT Haystack Observatory ⁷Applied Statistical Consulting

Abstract

We present a fully automated, deterministic technique for detecting and characterizing Large Scale Traveling Ionospheric Disturbances (LSTIDs) using 14 MHz amateur (ham) radio data. The method isolates wave periods between 1–5 hours and applies sinusoidal curve fitting to the first-hop skip-distance edge of observed communication ranges, yielding quantitative estimates of LSTID amplitude and period. Data from the Weak Signal Propagation Reporting Network (WSPRNet), the Reverse Beacon Network (RBN), and PSKReporter, which is now merged and available on the CEDAR Madrigal database, were used to produce a unified multi-year climatology of LSTID activity over the continental United States (2016–2023). Results show clear seasonal patterns: enhanced LSTID occurrence during winter, weaker activity in spring and fall, and modest summer increases. These results are consistent with prior studies and suggest modulation by neutral wind filtering, sudden stratospheric warming (SSW), vertical coupling, and solar activity.

Introduction

An amalgamation of amateur radio signals from distributed passive radio receiver networks provides a new tool for investigating characteristics of the complex ionosphere. This tool is voluminous, geographically widespread, and free. This work investigates some of its ambiguities.

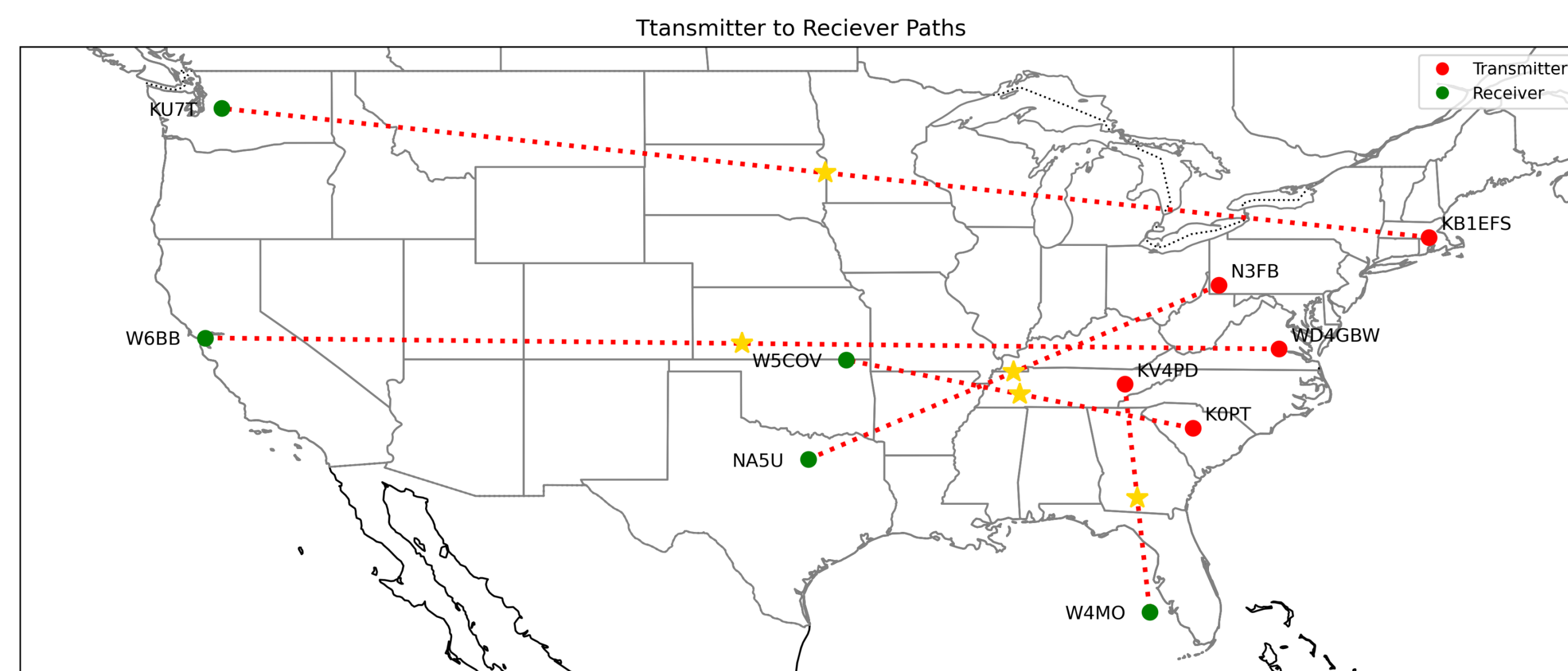


Figure 1: Example amateur radio transmitter–receiver paths across CONUS used for LSTID detection.

- Visually found quasi-periodic variations in the minimum HF signal distance within WSPRNet, RBN, and PSKReporter ham radio observations, yielding LSTID parameters.
- WSPRNet, RBN, PSKReporter are automated communication observation networks that are voluntarily operated by amateur radio operators that can monitor and log radio signals.
- Each datum ("spot") includes information on the transmitter, receiver, time, and frequency.

The relevant amateur radio operators (transmitter and receiver) were geofenced to be within the continental United States. It is assumed that their transmission was reflected off the ionosphere right above its midpoint. Tallies of these transmissions were gathered from RBN, WSPR, and PSK reporter databases on a one-minute cadence. These data were assembled into pixels 25 km wide. The range of 12 to 24 UTC and 0 to 3000 km resulted in 0 to 720 minutes by 0 to 120 pixels (86, 400 pixels in total). Our data was a plot of these spots, colored by the number of contacts in a pixel.

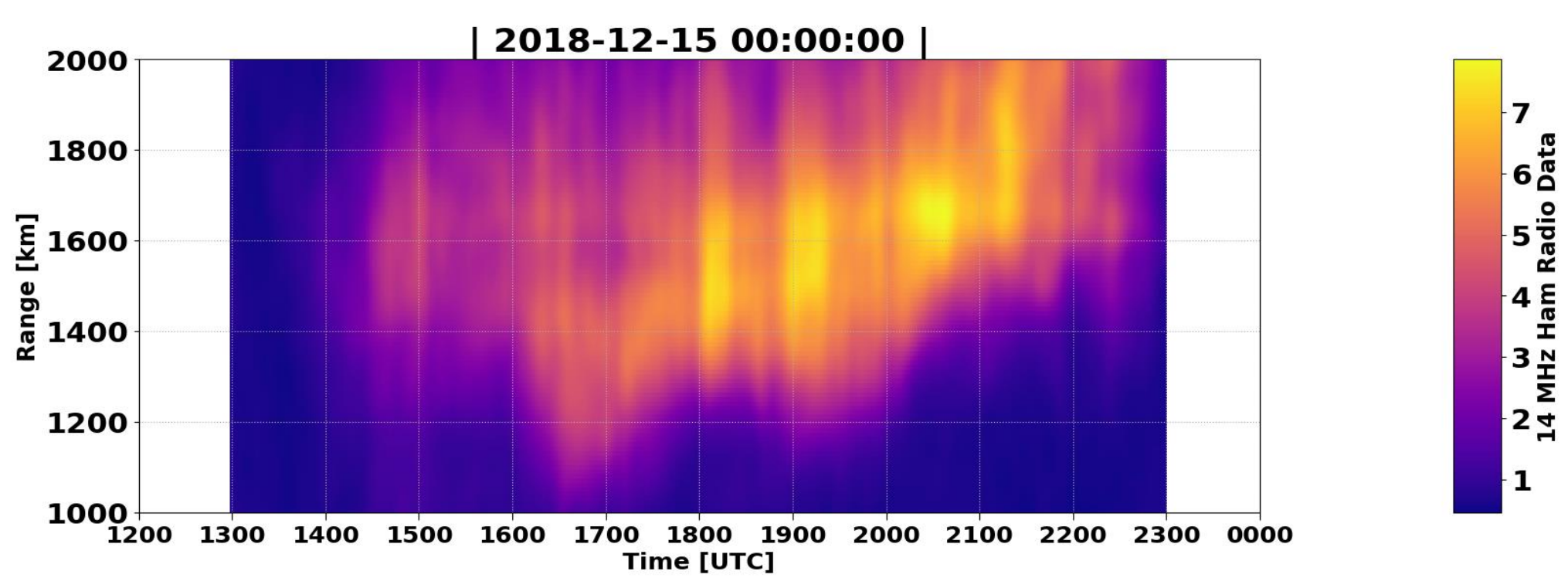


Figure 2: Pre-processed amateur radio histogram.

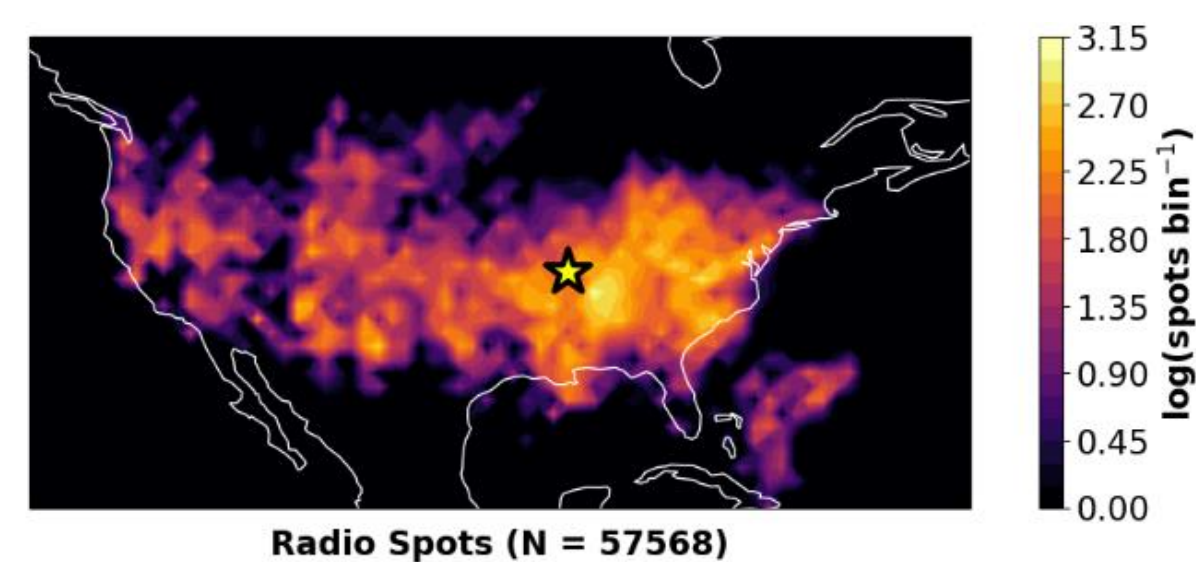


Figure 3: 2D Ham radio histograms generated from RBN and WSPRNet with geographic location of midpoints between transmitters and receivers.

Method

A deterministic and fully automated detection method was then developed to find these LSTID structures in the amateur ham radio spot data. Images are first trimmed to where LSTIDs are regularly observed. A function for median absolute deviation rescaling and gaussian blurring is then applied to help with edge detecting. For each discrete bin represented in the image, values lower than the bin are removed. This results in a minimum line tracking the edge for that threshold, the vertical values of minimum height measured data are stored in the corresponding bin.

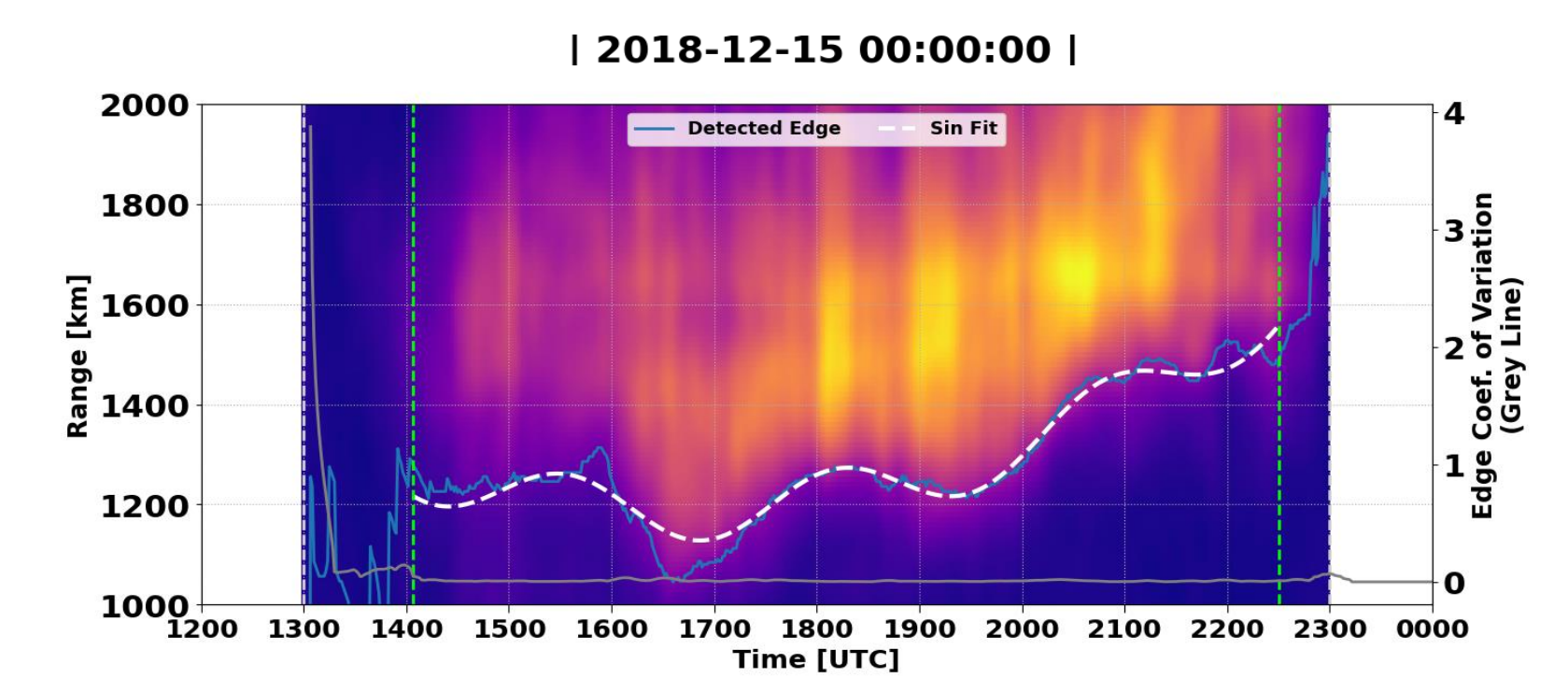


Figure 4: Preprocessed amateur radio histogram with detected edge, coefficient of variation, and curve fitting superimposed.

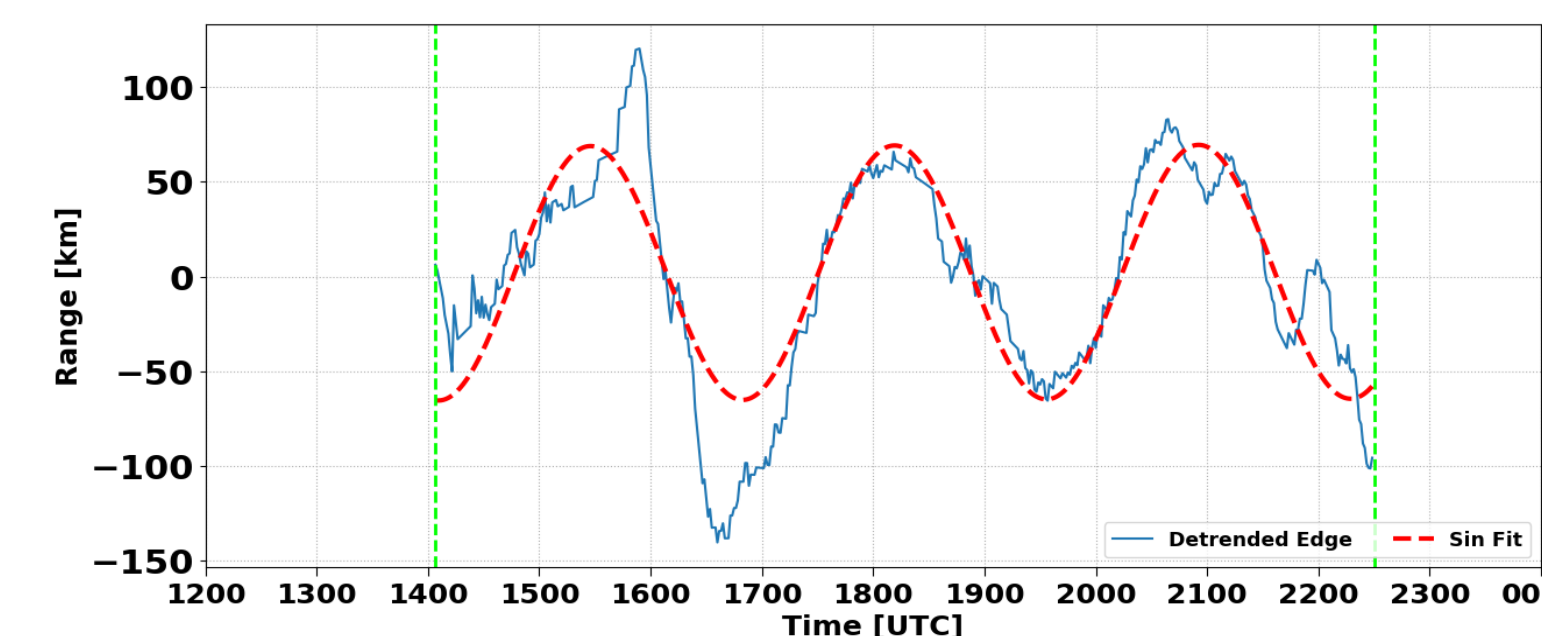


Figure 5: Detrended detected edge and sinusoid curve fit.

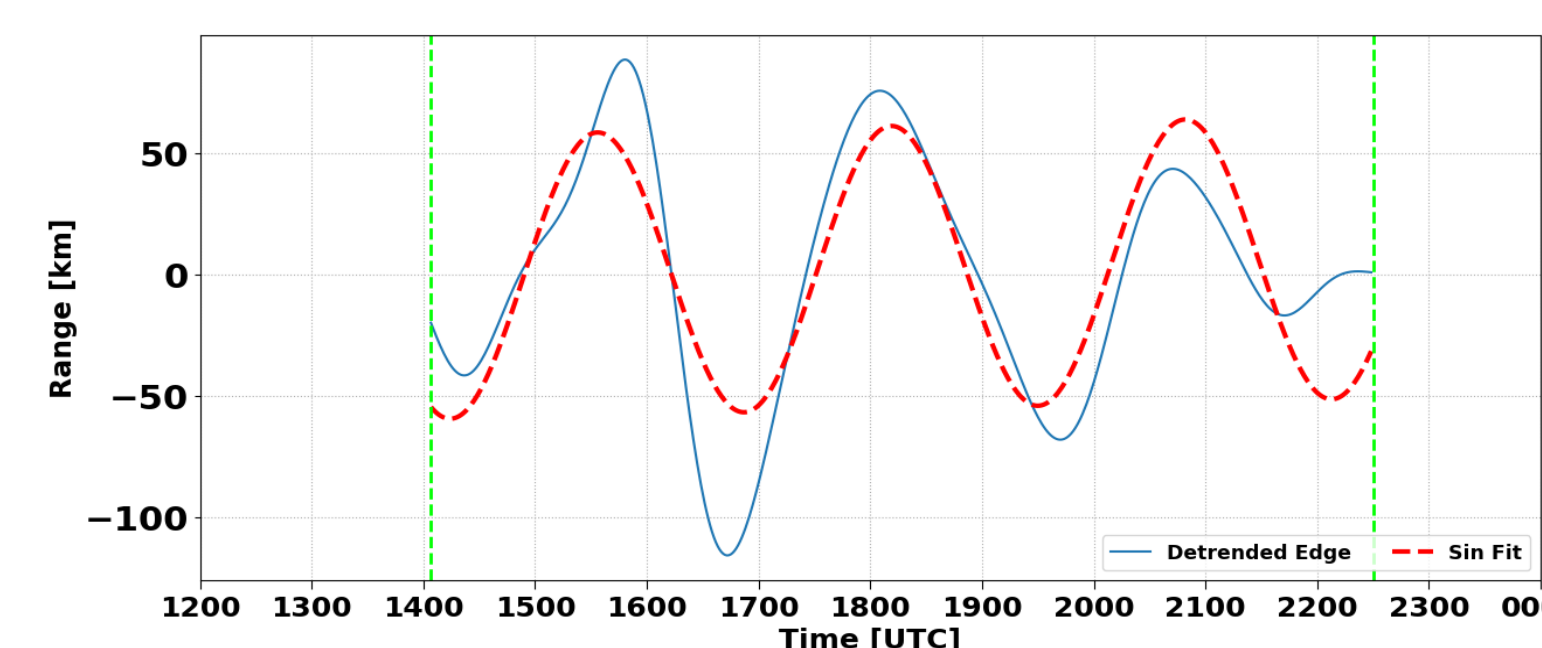


Figure 6: Detrended detected edge and sinusoid curve fit with band-pass filter.

Results

Automated sinusoidal fitting of daily HF propagation signatures was applied across CONUS for 2015–2022. Fitted amplitude shows a strong repeatable seasonal cycle with persistent winter enhancements and reduced summer amplitudes, with the seasonal envelope broadly tracking the Polar Vortex index. Periods of stronger vortex activity coincide with enhanced disturbance amplitudes. Minimum RF skip distance exhibits both seasonal structure and clear multi-year variability broadly following F10.7 solar flux, an inverse relationship consistent with solar-cycle modulation of F-region electron density. Elevated solar flux during solar maximum enhances F-region electron density, permitting steeper-angle refraction and shorter skip distances, while declining activity toward solar minimum produces the opposite effect.

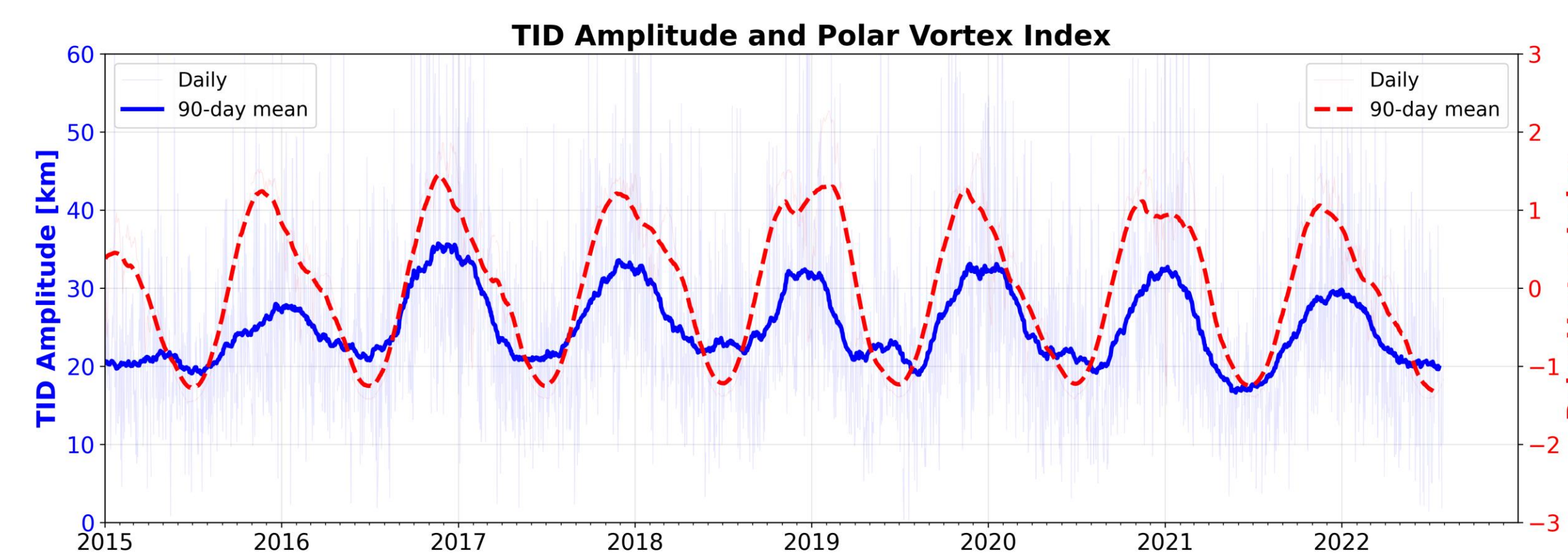


Figure 7: Daily and 90-day smoothed time series of fitted LSTID amplitude and Polar Vortex index, 2015–2022.

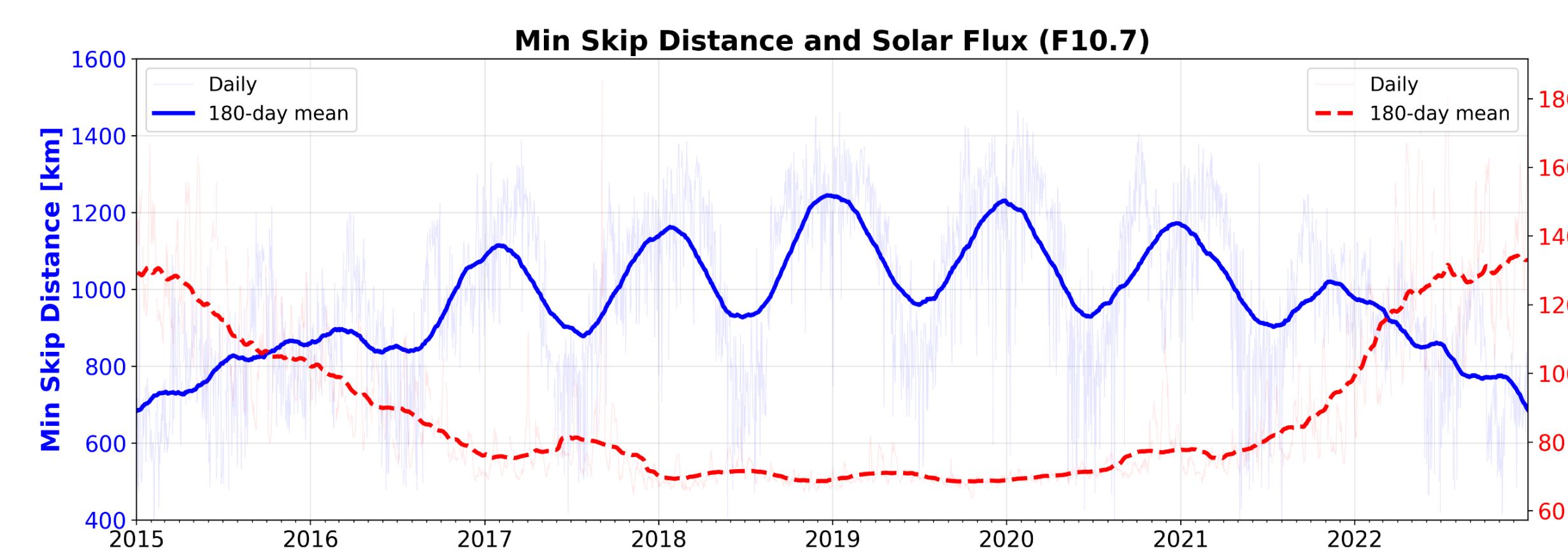


Figure 8: Daily and 90-day smoothed time series of minimum RF skip distance and F10.7 solar flux, 2015–2022.

LSTID Classification

A binary event classification was introduced to distinguish days with physically meaningful disturbance structure from days with only weak background variability. A day is designated LSTID-active when fitted amplitude ≥ 33 km, period between 1–5 hr, and $R^2 \geq 0.35$; all remaining quality-controlled days are designated calm. This threshold was selected by minimizing RMSE between automated and manual monthly occurrence fractions for 2017. The automated classification reproduces the independent manual seasonal cycle; enhanced occurrences fall through spring while being suppressed in summer.

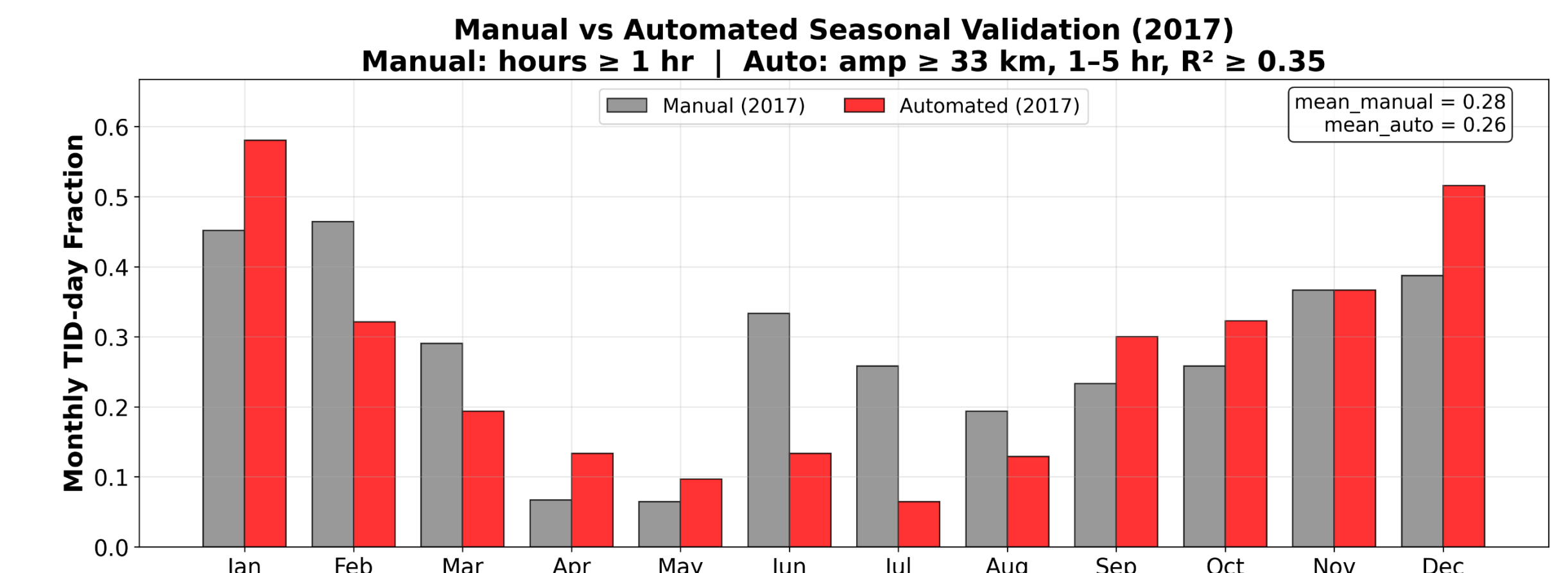


Figure 9: Monthly TID-day fractions for 2017 from manual (gray) and automated (red) classification at the 33 km threshold.

LSTID-active days occur preferentially during fall and winter while calm days dominate late spring and summer, with stable monthly sample sizes confirming this is not a sampling artifact. Conditional probability distributions show AE and SYM-H overlap strongly between LSTID-active and quiet days, indicating geomagnetic forcing does not explain the dominant seasonal structure. The Polar Vortex index shows the clearest separation; LSTID-active days are weighted toward more positive vortex values, consistent with stratospheric variability modulating the seasonal probability of LSTID occurrence. This result is robust across amplitude thresholds from 25–35 km.

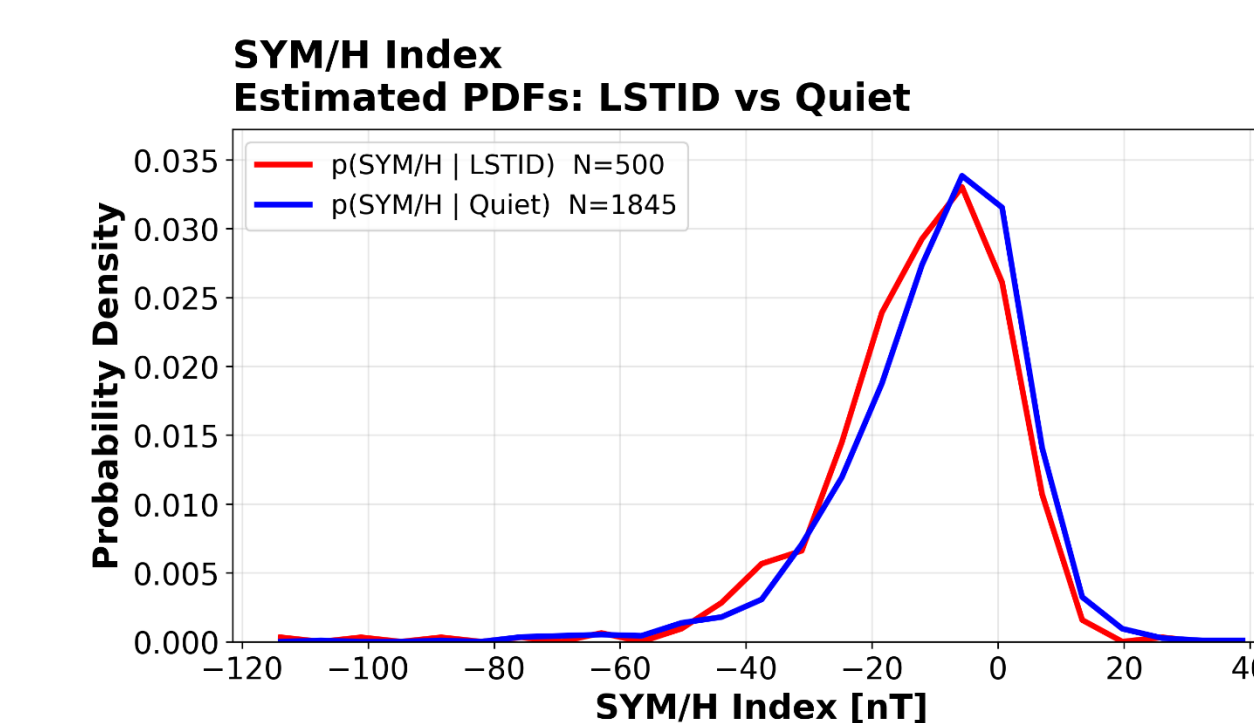
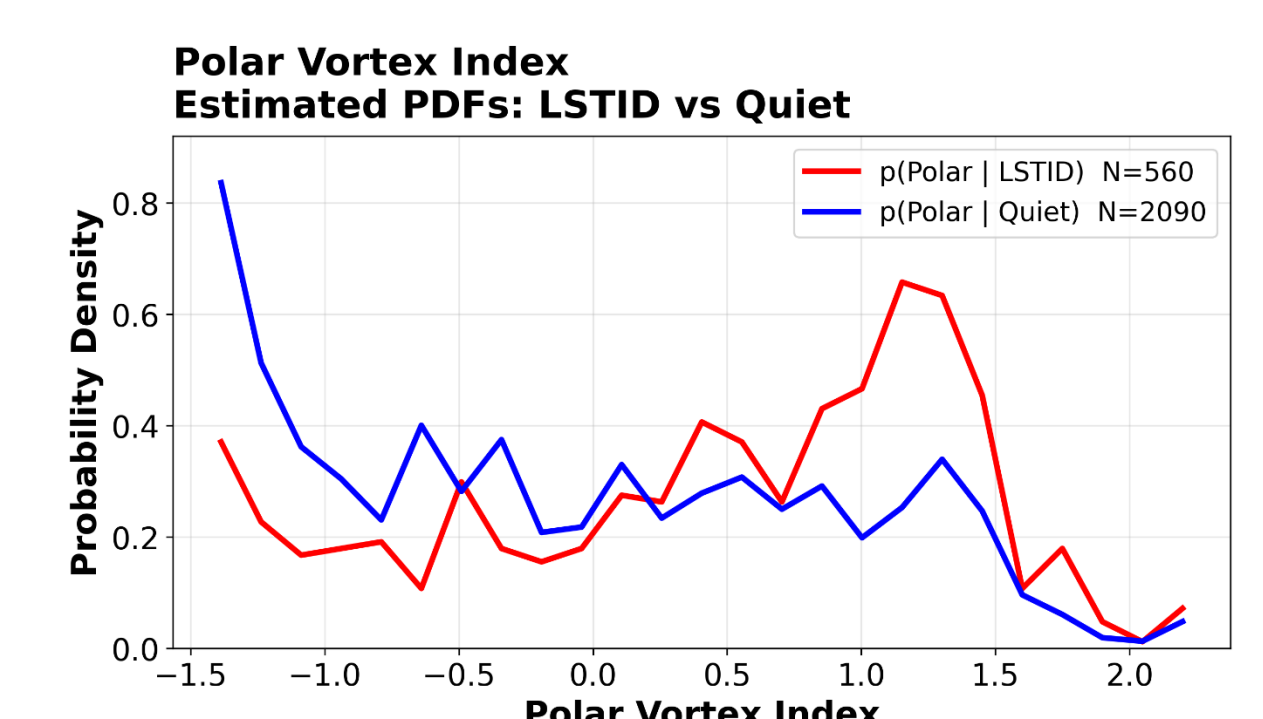
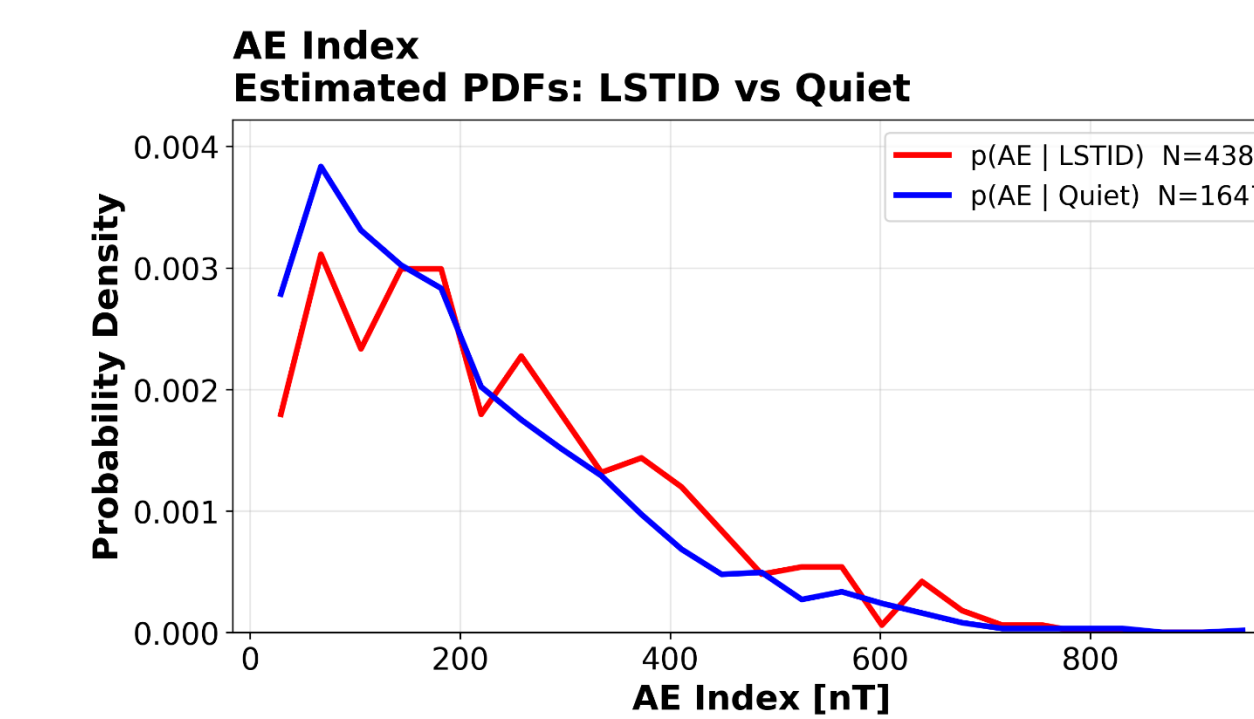


Figure 10: Conditional probability density functions for AE, SYM-H, and Polar Vortex index during LSTID-active (red) and quiet (blue) days, 2015–2022.

Conclusions

- LSTIDs occur mostly in fall and winter, with reduced activity in spring and summer.
- Minimum RF skip distance shows a clear inverse relationship with solar flux, consistent with solar-cycle modulation of F-region ionospheric conditions.
- Polar Vortex index shows the strongest separation between LSTID-active and quiet days, which most strongly explains the seasonal LSTID occurrence.
- Geomagnetic indices (AE, SYM-H) show strong distributional overlap between classes and do not explain the persistent seasonal structure.
- The automated detection framework reproduces independent manual classification results, validating the approach.

References and Acknowledgements

Frissell, N. A., Baker, J. B. H., Ruohoniemi, J. M., Gerrard, A. J., Miller, E. S., Marini, J. P., West, M. L., and Bristow, W. A. (2014). Climatology of medium-scale traveling ionospheric disturbances observed by the midlatitude Blackstone SuperDARN radar. *J. Geophys. Res. Space Physics*, 119, 7679–7697, doi:10.1002/2014JA019870.
 Frissell, N. A., Baker, J. B. H., Ruohoniemi, J. M., Greenwald, R. A., Gerrard, A. J., Miller, E. S., and West, M. L. (2016). Sources and characteristics of medium-scale traveling ionospheric disturbances
 We are especially grateful to the amateur radio community, especially the operators of the Reverse Beacon Network (RBN, reversebeacon.net), the Weak Signal Propagation Reporting Network (WSPRNet, wspnet.org), qrz.com, and hamcall.net. NAF is grateful for the support of NSF AGS-2045755, NASA 80NSSC21K1772, and NASA 80NSSC23K0848/1564031. We acknowledge the use of the Free Open-Source Software projects used in this analysis: Ubuntu Linux, python, matplotlib, NumPy, SciPy, pandas, xarray, iPython, and others.
 We would also like to make a special mention to Dr. Lynn Harvey of the University of Colorado Boulder for her contribution to this study and for facilitating the MERRA-2 data utilized in this climatology.